A Hybrid Object-based/Pixel-based Classification Approach to Detect Geophysical Phenomena

Xiang Li, Rahul Ramachandran, Sara Graves, Sunil Movva
Information of Technology and Systems Center
University of Alabama in Huntsville

ABSTRACT

Geophysical phenomena are observable events with spatio-temporal characteristics. These phenomena can have spatial extent and shape but the intensities are generally not homogeneous within this spatial extent. These phenomena also evolve, grow and perish over time. Therefore, developing a robust detection algorithm for geophysical phenomena is difficult and challenging. This paper presents a hybrid object-based/pixel-based classification methodology for shape-based geophysical phenomena detection from image data. The target phenomena for this study are the frontal systems in the atmospheric model-generated wind field data. The methodology is comprised of two levels of data mining. At the pixel-level, the image is soft classified pixel by pixel to calculate the probability that it is the component of the geophysical phenomena. The K-means clustering algorithm is used to create this soft classification. At the object-level mining, a hierarchical thresholding technique is coupled with a Gaussian Bayes classifier to optimally segment the individual regions of interest. At each hierarchical level, the probability image is segmented and shape factors are calculated for the segmented regions. The optimal threshold for a region is the one that produces the maximum likelihood from a Gaussian Bayes classifier based on the shape factors of the region. The object level mining is followed by post processing to filter false signatures. Experimental results show that this methodology effectively detects the frontal systems in the model data and the detected regions are in good agreement with the ones identified by the domain experts. This hybrid methodology can be applied to detect other geophysical phenomena in science datasets.

1. INTRODUCTION

Supervised classification has been widely used for event detection and scene classification of remote sensing data in the Earth Science domain. For example, artificial neural networks were used to classify cloud and scene types [1] and to detect fire and smoke events [2] in satellite imagery. These geophysical phenomena can be properly identified based on the spectral and textural properties of satellite images at the pixel scale. In other words, the classification is done pixel by pixel. However, some geophysical phenomena, such as frontal systems and cyclones, have distinct shape characteristic. Characterization of these phenomena depends not only on their statistical properties but also on their morphological properties. Pixel-based classifiers have difficulty in detecting such geophysical phenomena. Instead, the detection of these phenomena has to be accomplished at the higher object level.

This paper presents a hybrid object/pixel-based classification methodology for automated detection of shape-based geophysical phenomena from Earth Science data. These geophysical phenomena are observed as objects or regions of interests in Earth Science data. Carmichael and Hebert presented a technique that combines pixel-level and object-level approaches into a unified framework for shape-based object recognition [3]. The framework was targeted for computer vision applications. In pixel-level phase, each pixel was classified based on the spatial arrangement of edge features in its local neighborhood. In object-level phase, an overall score for a region were determined as the sum of the classification scores for all pixels in the region. High score regions represented the candidate regions for target objects. The coupled pixel/object phase processing was recursively applied to the candidate regions to narrow down and detect target objects. Our proposed methodology follows their concept of combining pixel-level and object-level mining. However, the mining techniques used at both levels are different from [3] because of the different problem domain. At the pixel-level, an unsupervised K-means clustering algorithm is first applied to feature samples to partition the feature space into a number of clusters. Domain knowledge is then used to determine which clusters most probably represent the phenomena of interest. The probability that a cluster belongs to the phenomena of interest is calculated for each image pixel using the clustering result. This is referred to as soft classification. The soft classification at pixel-level mining allows the object-level mining step to aggregate target pixels into optimal regions and determines the optimal threshold based on the high-level shape factors. Thus, at the object-level mining, a hierarchical thresholding technique is applied to the generated probability image to extract the regions of interest as phenomena. At each hierarchical level, the image is segmented and shape factors are calculated for the segmented regions. The optimal threshold for a region is the one that produces the maximum likelihood from a Gaussian Bayes classifier based on the shape factors of the region.

In this study, this hybrid object-based/pixel based methodology was used to extract frontal systems from Atmospheric Model-generated wind fields. A front is a narrow transition zone at mid-latitudes where two air masses with significantly different properties meet. Fronts are often observed as elongated or comma-like curve regions in Atmospheric Model outputs. Section 2 provides a description of the Atmospheric Numerical Model data used in this study. Section 3 describes the hybrid methodology for geophysical phenomena detection and extraction. Section 4 shows the experimental results and discussions. Finally, conclusions are presented in Section 5.

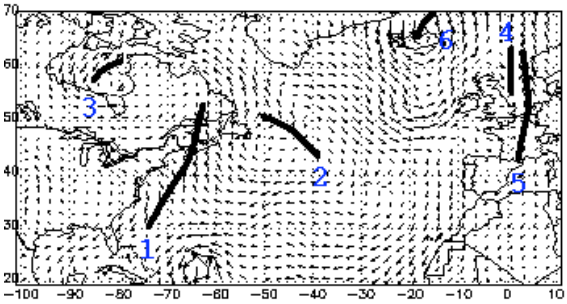

Figure 1 Surface wind field from fvCCM model output at 09/12/00Z, 1999. Solid lines indicate identified front locations.

2. DATA

The output from the Goddard Laboratory of Atmosphere's finite volume Community Climate Model (fvCCM) was used in the study. The output data fields have a horizontal resolution of 0.5 ° Latitude x 0.625 ° Longitude with a vertical resolution of 36 levels including the surface. The output data fields were generated 4 times daily (every 6 hours). The data fields used in this study were the surface wind and potential temperature fields from September 12, 1999 to September 19, 1999 and a total of 31 data sets, corresponding to 31 time steps during this time period were available. The area of study is 20°N - 70°N Latitude and 100°W - 10°E Longitude. Figure 1 shows the surface wind field at September 12, 00Z Universal Time (UT). The solid lines in the figure represent the locations of frontal systems as identified by the domain experts and the numbers are the front indices. These frontal system locations are considered as the "truth" data and are used to evaluate the hybrid methodology. The ground truth information covered 8 time steps between September 12, 00Z and September 13, 18Z.

The original U and V wind fields were used to derive four features that were then utilized for mining. Two of the features used were vorticity and confluence and they characterize different aspects of the wind flow patterns. Vorticity is helpful in identifying the veering of wind direction change where as confluence characterizes the convergence zone of wind field. The third feature used was the wind direction variation (WDV) which captures the wind direction change at a grid and was determined by the wind fields of its local neighbors. Combined with the wind speed, these four features were used to characterize a weather front. Li et al. presented the detailed descriptions of these features [4].These features were calculated for each model grid point and grouped as a feature vector. Each point in the 4-dimensional feature space was represented by a feature vector.

3. METHODOLOGY

The proposed methodology for shape-based geophysical phenomena detection is the combination of low-level pixel-based and high-level object-based mining. The basic idea is to identify all the data points that represent the phenomena at the pixel level and group these pixels into regions and to classify the candidate regions at higher object-level using shape information.

3.1 Pixel-level Mining

Pixel-level mining is typically used to classify individual pixel whether it is a component of geophysical phenomena or not. Supervised classification is the most common approach for this purpose. After selecting a classifier, truth data are used to train and test the classifier for optimal classification performance. The trained classifier is then used to classify a pixel into a certain type. The output from such a classifier is normally binary, i.e., one class for a pixel. This is called hard classification. For shape-based geophysical phenomena detection, the region of interest is determined at higher object-level based on the region's shape information. As a result, hard classification of each pixel leaves little room for higher object level decision making and can worsen the overall performance. Instead, soft classification can be used to estimate the probability whether a pixel belongs to the class of interest or not. Soft classification can be accomplished using unsupervised K-means or fuzzy C-means clustering algorithms. In this study, we use K-means clustering algorithm for soft classification.

We assume that the distribution of feature vectors for front and non-front pixels are significantly different. Consequently, they form clusters at different regions of the feature space. The K-means algorithm is used to partition this feature space into individual clusters in order to identify the clusters that represent frontal system. A feature vector data set was generated from the wind field at 09/18/00Z and 09/19/00Z for K-means clustering. These two time steps were randomly selected and the feature vector data set contained both frontal and non-frontal vectors.

Since the number of cluster 'k' is a predefined parameter in the K-means algorithm, the value of k was determined using following iterative heuristic approach. The k value was iteratively incremented and the overall root-mean-square (RMS) error was calculated. The error decreased monotonically with increasing k value and the final k value selected was the smallest number at which the decrease of relative RMS error was less than 1%. The k number selected was 19. From domain knowledge, we know that the frontal system generally has the following properties: moderate to high values in wind speed; vorticity; confluence; and wind direction variation. As a result, the clusters 6, 7, 8, 11, and 18 are labeled as the ones representing the features of frontal systems.

Assuming that the feature space is properly partitioned into clusters using K-means algorithm, we can now perform soft classification for each grid feature based on the membership function used in the Fuzzy C-means clustering. A membership vector M was calculated for a feature vector based on the distance of the feature vector to each of the cluster centers. The size of the membership vector is K and each vector element M_i represents the probability that the feature vector belongs to the ith cluster center. Based on the soft classification, a probability image is generated where the value of an image pixel is the probability that it belongs to a frontal system and is determined as the summation of the membership elements corresponding to the front clusters (clusters 6, 7, 8, 11, and 18). Results show that the regions identified as frontal systems by the experts coincide well with the high intensity regions in the probability image.

3.1 Object-level Mining

The object-level mining step has two objectives and these are: 1) to identify candidate regions; and 2) to justify that the extracted regions represent the geophysical phenomena. The object-level

mining step groups the pixels into regions which are most likely to be the geophysical phenomena of interest and spatially connected. These regions are then classified as the geophysical phenomena based on their shape factors. The intuitive approach would be to apply a simple global thresholding algorithm to the probability image generated at pixel-level phase and form regions using a region growing algorithm. However, the probability values may be quite varied for different regions with different signature intensities. It may not be possible to properly detect all regions of phenomena of interest using a single global threshold. If threshold value is set too low, the detected region may be too large and consequently the shape factors values get skewed. If threshold value is set too high, a region of interest may be broken into pieces or not be properly detected. Therefore, instead of global thresholding, a hierarchical thresholding technique was used for object extraction. The advantage of hierarchical thresholding allows one to obtain optimal threshold for each region of interest.

Since, fronts normally appear as elongated strips or curves due to their narrow transition zones, a region can be identified as frontal or non-frontal regions based on its shape. We used the following eight shape descriptors based on the region and its convex hull [5]: 1) perimeter of the region; 2) area of the region; 3) perimeter of the convex hull of the region; 4) area of the convex hull of the region; 5) aspect ratio of the region, defined as the square of the region perimeter divided by the four times the area of the region; 6) the ratio of the two principle axes of the region [6]; 7) ratio of the perimeter of the region to the perimeter of its convex hull; and 8) ratio of the area of the region to the area of its convex hull. A Gaussian Bayes classifier was trained to classify the front regions based on these shape descriptors. The sample data set to train and test the Bayes classifier was generated from the model data for several time steps by hierarchical thresholding the probability images and the domain expert labeling each detected region. This data had a total of 1045 samples with 386 samples labeled as fronts. The generated sample data set was randomly split into two subsets; one for training classifier and the other for testing classifier performance. The training subset had a total of 563 samples while the testing subset had total of 482 samples. The accuracies of training and testing set were 90.2% and 91.5%, respectively. The overall accuracy of the shape classifier was 90.8%.

3.3 Post processing

Besides the two major mining steps, a post processing heuristic algorithm to filter out the erroneously detected regions of interest and to smooth the region boundaries was applied. The heuristic filtering algorithm was based on domain knowledge. For example, since a frontal system is a transition zone of two significantly different air masses and large temperature gradient expects to be observed in the narrow front zone. This domain knowledge can be exploited to justify the frontal systems detected. In this study, the standard deviation of the potential temperature field (STD_PT) is used to further justify whether a region was correctly identified as a frontal system. If the STD_PT value of a region over water surface is less than 0.9 K or the region over land surface is less than 1.5 K, the identified frontal region was relabeled as a non-frontal system and filtered out. The differences in potential temperature criteria over land and water are important because the temperature over oceans tends to be more uniform than that over land surfaces; and the surface temperature has large impact on the air mass temperature. Our experiments show that by applying these rules, a couple of regions erroneously labeled as frontal systems were filtered out.

A morphological closing operation [6] was further applied to clean up the frontal systems detected by smoothing the boundaries of the fronts and filling the holes in the front regions. The template size used for the closing operation is 3 x 3. The smoothed frontal regions are then thinned using the Zhang-Suen algorithm [7] to obtain the skeletons of the frontal systems.

4. RESULTS

This hybrid methodology was applied to all 31 data sets for frontal system detections, of which the truth data was available from 09/12/00Z to 09/13/18Z. There were total of 34 frontal systems identified by the experts in these 8 time steps. Figures 2a, 2c, 2e, and 2g show the wind field and expert labeled frontal systems at the time steps of 00Z and 12Z of 09/12, and 00Z and 12Z of 09/13, respectively. Figures 2b, 2d, 2f, and 2h show the detected frontal systems at these corresponding time steps.

Fronts with indices 4 and 5 in Figures 2a and 2c are counted once at each time step since they are too close to each other and are detected as a single frontal system by our method. Our method detects 27 of the 34 frontal systems and the detection rate is 79.4%. The major frontal system at the east coast of the U.S., which is indexed as 1 in these figures, is precisely detected by the methodology at each of the time steps. This methodology also detects the other major frontal system, indexed as frontal system 9 in the figures, which moves across from the West to the East of the U.S. In addition, our methodology detects this frontal system at the early stage of its development at 09/12/00Z that was not identified by the domain experts. Experts did not identify this front at this time step because it is located at the boundary of the area of the study. Front with index of 7, located at southwest of the Greenland, is missed by our methodology at 09/13/00Z, though part of the frontal system is detected at its two adjacent time steps, 09/12/18Z and 09/13/06Z. The methodology did not identify the front at 09/12/00Z over the north of the Iceland, which has front index of 6 in Figure 2a. Also, the front over the northeast of Canada, which is indexed as 8, was not detected at time steps 09/12/06Z, 09/12/12Z, and 09/13/00Z. However, it is identified at time steps 09/12/18Z and 09/13/06Z. This is a weak front compared to fronts 1 and 9. Our methodology misses these frontal systems because of their weak shape descriptors. Our methodology also incorrectly detects regions over Spain and northwest of Africa. This was attributed to the wind conditions due to orographical effects. Special treatment and additional information are needed to filter out such false signatures.

5. CONCLUSION

A hybrid object-based/pixel-based classification methodology for shaped-based geophysical phenomena detection is presented in this paper. The hybrid methodology takes advantage of data mining at both levels. The low pixel-level mining evaluates each individual pixel the probability to be a component of the geophysical phenomena. The K-means clustering is used to create this soft classification. At object-level mining, hierarchical thresholding algorithm is applied to the probability image to determine optimal threshold for each region of interest in the image. The optimal threshold is justified by calculating the shape

factors of the region and feeding it to a Gausian Bayes classifier. The optimal threshold for a region is the one at which a Gaussian Bayes classifier score the highest.

The methodology was used to extract frontal systems from atmospheric model-generated output. Due to the significant variation of wind patterns in the front zones, automated detection using traditional pixel level based data mining approaches is difficult. In addition to the two levels of mining for front detection, rules derived using domain knowledge were used to further filter out the false signatures. Experiments results show that this hybrid methodology is effective in extracting frontal systems and can be applied to other similar shape-based geophysical phenomena.

ACKNOWLEDGEMENT

This work was funded by Ames Research Center and Goddard Space Flight Center, NASA grant NAG5-13263. The authors would like to acknowledge: David Emmitt and Steven Greco of Simpson Weather Associates; Robert Atlas of Goddard Space Flight Center, NASA; Joe Terry and Juan Carlos Jusem of Science Applications International Corporation for providing the data and the domain expertise.

REFERENCES

[1] Lee, J., R. C. Weger, S. K. Sengupta, and R. M. Welch, A neural network approach to cloud classification, IEEE Trans. on Geoscience and Remote Sensing, Vol. 28, pp 846-855, 1990

[2] Li, Z., A. Khananian, R. H. Fraser, and J. Cihlar, Automatic detection of fire smoke using artificial neural networks and threshold approaches applied to AVHRR imagery, IEEE trans. on Geoscience and remote sensing , Vol. 39, pp 1859-1870, 2001

[3] Carmichael, O. and M. Hebert, A hybrid object-level/pixel-level framework for shape-based recognition, Proceedings of British Machine Vision Conference, (BMVC), 2004

[4] Li, X., R. Ramachandran, S. Graves, S. Movva, B. Akkiraju, D. Emmitt, S. Greco, R. Atlas, J. Terry, and J.-C. Jusem, Automated detection of frontal systems from numerical model-generated data, the *11th ACM SIGKDD Inter. Conf. on Knowledge Discovery and Data Mining*, Chicago, U.S.A., August 21-24

[5] Gonzalez, R.C., and Woods, R.E. Digital image processing, *Addison-Wesley Publishing Company, 1992, 716pp.*

[6] Luo, T., Kramer, K., Goldgof, D.B., Hall, L.O., Remsen, A., and Hopkins, T. Recognizing plankton images from the shadow image particle profiling evaluation recorder, *IEEE Trans. On Sys. Man and Cyber., part B:Cybernetics, Vol., 34, No. 6, 2004.*

[7] Zhang, T.Y., and Suen, C.Y. A fast parallel algorithm for thinning digital patterns, *Comm. ACM, vol. 27, no. 3, 1984, pp236-239.*

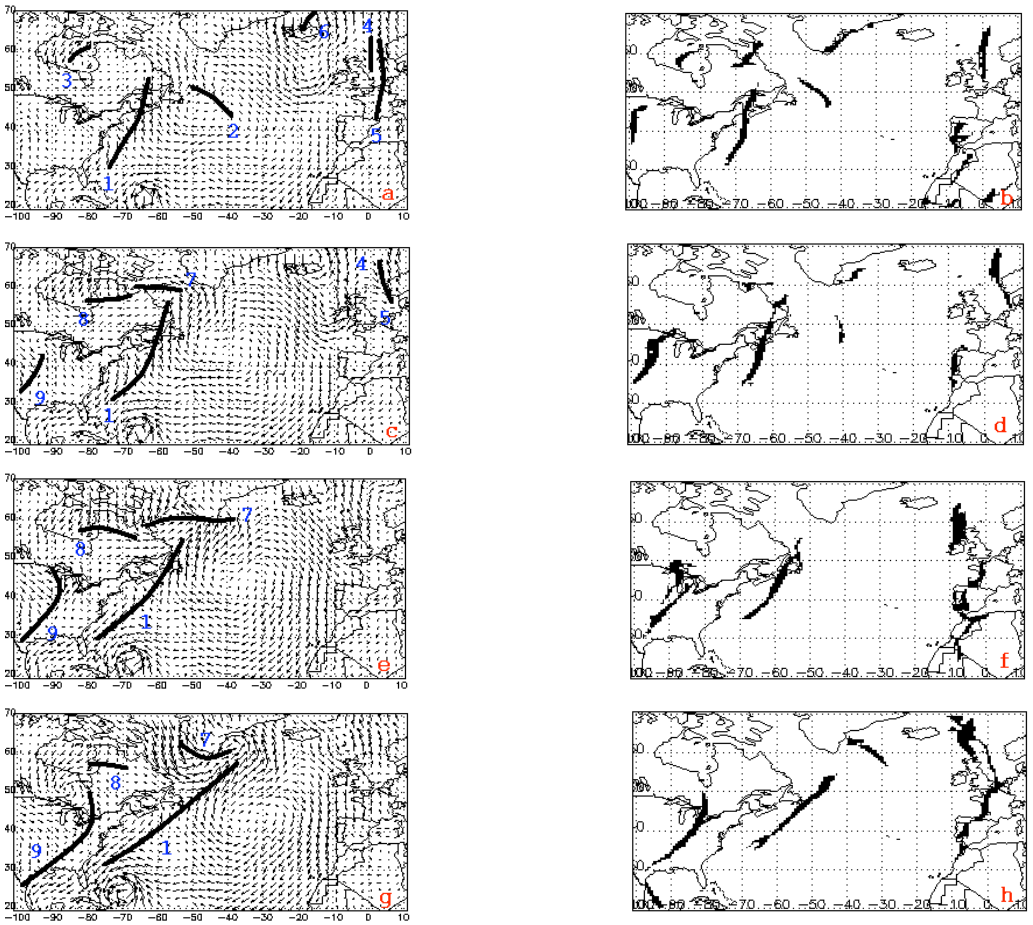

Figure 2 (a) – (h) Comparisons of frontal systems detected using the automated data mining method with the ground truth frontal systems identified by the domain experts. (a), (c), (e), and (g) show the ground truth fronts at 09/12/00Z, 09/12/12Z, 09/13/00/Z, and 09/13/12Z, respectively. (b), (d), (f), and (h) show the automatically detected frontal systems at 09/12/00Z, 09/12/12Z, 09/13/00Z, and 09/13/12Z, respectively.